International Journal of Geo-Energy

Int.J.Geo-Energy.2023.1(1).0001
ISSN：2958-2857
https://doi.org/10.58531/ijge103100002

Article

Research on Drilling Test of Grouting Rock Mass Based on Cutting Strength

Wansheng Chen [1], Hongke Gao [2,*], Hui Liu [1], Fei Chen [1], Yuxiang Cao [1], Fenglin Ma [2], Chun Zhu [3], Songlin Cai [2] and Jiajie Li [4]

[1] Shenmu Ningtiaota Coal Mining Company Ltd, Shaanxi Coal and Chemical Industry Group Company Ltd., Yulin, Shaanxi 719300, China
[2] Stake Key Laboratory for GeoMechanics and Deep Underground Engineering, China University of Mining and Technology-Beijing, Beijing 100083, China
[3] School of Earth Sciences and Engineering, Hohai University, Nanjing 210024, China
[4] School of civil and resource engineering, University of Science and Technology Beijing, Beijing 100083, China
*Corresponding author: Hongke Gao< ghk@cumtb.edu.cn>

Academic Editor: Prof. Krzysztof Skrzypkowski < skrzypko@agh.edu.pl>

Received: 19 April 2023; Revised: 16 May 2023; Accepted: 18 May 2023; Published: 20 May 2023

Abstract: Grouting is an effective way to control the fractured surrounding rock in underground engineering. Quantitatively obtaining the strength parameters of grouting rock mass is very important for the grouting parameters rational design. Drilling tests of grouting rock masses with different water-cement ratios and particle sizes are carried out using the rock digital drilling test system. Based on the rock cutting mechanical model, the cutting strength of grouting rock is obtained. The response laws of different water-cement ratios and rock particle sizes on drilling parameters, cutting strength, and strength parameters are analyzed. On this basis, combined with the analysis of the relationship between grouting sandstone specimens' strength and drilling parameters with different water cement ratios, a while-drilling testing model of grouting rock mass strength parameters based on cutting strength is established. It is a theoretical basis for quantitatively evaluating the strength of grouting surrounding rock while drilling in underground engineering.

Keywords: rock test while drilling; compressive strength; cutting strength; quantitative evaluation

Citation: Chen W, Gao H, Liu H, Chen F, Cao Y, Ma F, Zhu C, Cai S, Li J. Research on Drilling Test of Grouting Rock Mass Based on Cutting Strength. Int. J. Geo-Energy, 22023, 1(1), doi: 10.58531/ijge103100002

1. Introduction

With the continuous development of the depth and breadth of underground engineering, many complex geological conditions appear. Loose and broken rock mass leads to the failure of support structure easily, and engineering disaster problems such as roof collapse, floor heaving and sidewall spalling occur frequently [1-3]. As primary control means of fractured surrounding rock, grouting can improve the fractured surrounding rock mechanical properties [4-6]. It can improve the integrity of surrounding rock and bearing capacity effectively and is widely used in underground engineering fields [7-9].

The real-time evaluation of grouting reinforcement effect is essential for the design and optimization of supporting scheme such as advanced pre grouting and bolt-grouting support [10, 11]. The important way to evaluate the grouting reinforcement effect is to measure the grouting rock mass strength. Relevant scholars have studied the rock mass strength and test methods. In terms of indoor test, Zong and Han [12] obtained the variation law of strength before and after reinforcement through uniaxial compression test of rock mass, and analyzed the influence of confining pressure on the strength of grouted rock mass. Sun et al. [13] obtained the variation law of grouting rock parameters such as the rock mass cohesion and internal friction angle before and after grouting through indoor tests. Lu and Zhang [14] obtained the grouting rock parameters such as rock mass normal stiffness and shear strength before and after reinforcement through shear test. Salimian et al. [15] obtained shear strength of grouting rock through shear test, and analyzed the grouting impact with different water-cement ratio on rock mass strength parameters. Indoor tests are mainly carried out through uniaxial compression, triaxial compression and other tests on grouted rock mass. It is difficult to obtain the strength parameters of grouting surrounding rock in situ quantitatively, and then it is impossible to evaluate the grouting effect of surrounding rock in real time.

Therefore, some scholars have studied the field test evaluation method of grouted rock mass. Wang et al. [16] analyzed the grouting effect through the hydraulic discharge of drilling holes. Lin et al. [17] used the acoustic wave detection method to obtain the acoustic wave velocity of the grouting surrounding rock, and evaluated the grouting effect through the magnitude of wave velocity. Chen et al. [18] analysed the relationship between the grouting surrounding rock strength and wave velocity. Wang et al. [19] used analytic hierarchy process to evaluate the grouting effect in fault fracture zone, and to evaluate the grouting effect by using fuzzy comprehensive evaluation method. At present, the on-site evaluation mainly evaluates the grouting effect of rock mass through acoustic wave detection, drilling holes coring, borehole inspection and other methods. The surrounding rock needs to be drilled before test with these methods. The test process is cumbersome and the test range is limited. A simple and real-time method for the strength evaluation of grouted rock mass is needed.

Many studies have indicated that the drilling parameters can be obtained through the rock mass drilling process, which is related to the rock mass strength [20-24]. Chen and Yue. [20] proposed a zoning analysis method based on fragmentation by analyzed on-site rotary impact instrument drilling monitoring and related data. He et al. [21] conducted experimental research on the response characteristics of drilling energy to rock discontinuity using drilling

methods, and proposed an empirical method to determine the relationship between rock quality index (RQD) and drilling energy changes. Wang et al. [22] established a rock cutting mechanics model and derived the ultimate cutting force of the rock, obtaining the drilling parameters DP (Drilling Parameters) and rock c-φ parameter relationship. It provides a new way to evaluate the grouting rock mass strength in the drilling process. It is important to establish the quantitative relationship between the grouting rock mass strength and the drilling parameters.

In this paper, the drilling tests of rock mass reinforced by cement slurry are carried out by the self-developed digital drilling test system. The cutting strength of rock mass is obtained based on cutting mechanical model. The response law of cutting strength and compressive strength to different water-cement ratio and rock particle sizes are analyzed. The drilling testing model of strength parameters of grouting rock mass based on cutting strength is obtained. It can provide a theoretical basis for the drilling quantitatively evaluating the grouted surrounding rock strength in underground engineering.

2. Rock drilling tests

2.1. Test instrument

The digital drilling tests with the self-developed digital drilling test system are carried out [25]. This system was developed by the author's team, as shown in Figure 1. This system can control and monitor drilling parameters while drilling. The system has two control and monitoring modes: ①Control the drilling rate V_s and rotational speed N_r, and monitor the drilling torque M_q and drilling pressure F_p; ②Control the drilling pressure F_p and rotational speed N_r, and monitor the drilling rate V_s and drilling torque M_q. The lateral confining pressure with the maximum load of 1000kN can be applied to the rock specimen. Therefore, the digital drilling test with multiple control modes can be achieved. The bit used in the test is a new type of PDC drill bit. The square composite piece of cutting edge is in linear contact with the rock. It is easy for analysis of rock cutting process at the same time.

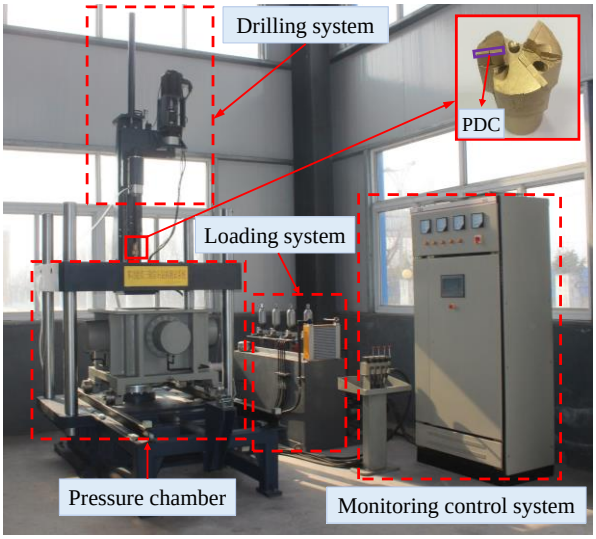

Figure. 1 Rock digital drilling test system and digital analytical drill bit

2.2. Test schemes

To analysis the relationship between drilling parameters and strength parameters, the drilling test of grouting rock mass reinforced by cement slurry is carried out. The sandstone used in the test is taken from a deep mine. The crushed sandstone is divided into 5~10mm, 10~15mm, 15~20mm, 20~25mm and 25~30mm, with a total of 5 rock particle sizes. The fractured sandstone is cemented by cement mortar. The sandstone with different particle sizes is made into cuboid specimens with length × width × height =150×150×200 mm.

The gradients of different water-cement ratio specimens are 0.4, 0.5, 0.6, 0.7 and 0.8 respectively, the particle sizes are 10-15mm, and the specimens are numbered G11-G15. The gradients of different rock particle sizes are 5-10mm, 10-15mm, 15-20mm, 20-25mm and 25-30mm, the water-cement ratio is 0.5, and the specimens are numbered G21-G25. At the same time, the same proportion of rock specimen is made to test the compressive strength. The scheme of specimen is shown in Table 1. In the digital drilling test, Vs and Nr are set to 80 mm/min and 100 r/min, respectively. The specimen after drilling is shown in Figure 2.

Table 1 The scheme of rock mass reinforced by cement slurry.

Specimens number	Water-cement ratio	Rock particle sizes /mm
G11	0.4	10-15
G12	0.5	10-15
G13	0.6	10-15
G14	0.7	10-15
G15	0.8	10-15
G21	0.5	5-10
G22	0.5	10-15
G23	0.5	15-20
G24	0.5	20-25
G25	0.5	25-30

Figure. 2 Rock mass reinforced by cement slurry after drilling

2.3. Test results

2.3.1. Selection method and result of drilling parameters

The drilling test can obtain four kinds of drilling parameters in real time: drilling rate V_s, drilling pressure F_p, rotational speed N_r and drilling torque M_q. Taking specimen G13 as an example, the curves of M_q and F_p with drilling depth are shown in Figure 3 and Figure 4. When the cutting edge contacts the specimen, M_q and F_p increased rapidly. M_q and F_p fluctuated near a stable value with the depth increases. The drilling process can be divided into rapid increasing stage and stable fluctuation stage.

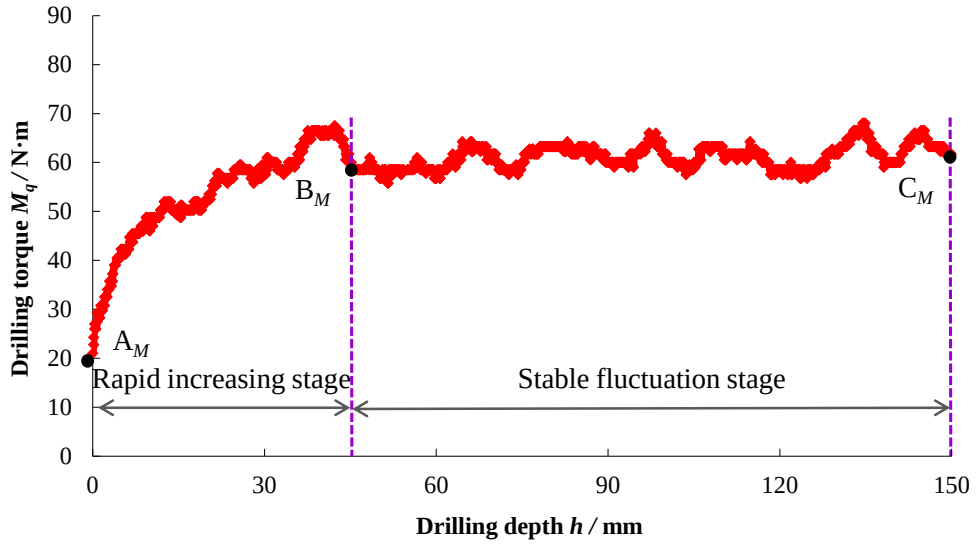

Figure. 3 Variation curve of drilling torque M_q with drilling depth.

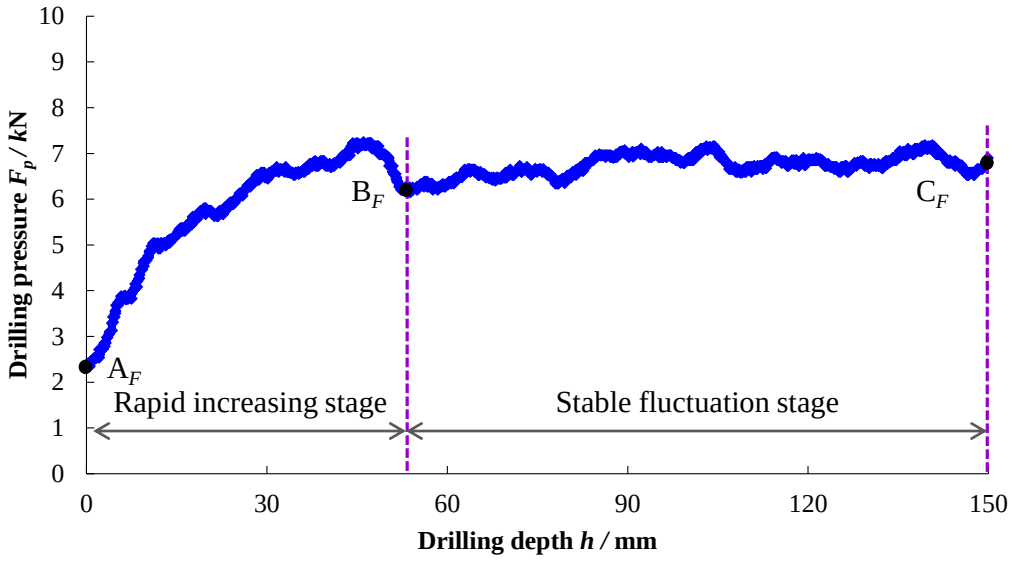

Figure. 4 Variation curve of drilling pressure F_p with drilling depth.

In the experiment, V_s and N_r are the average values of the stable fluctuation stage. M_q and F_p are the average value of the stable fluctuation stage minus the initial value of the rapid increasing stage. The drilling parameters and compressive strength of different water-cement ratio and different particle sizes grouting rock mass are shown in Table 2.

Table 2 Drilling test results of slurry reinforced rock mass.

Specimens number	V_s (mm/min)	N_r (r/min)	M_q (N·m)	F_p (kN)	σ_c (MPa)
G11	82.59	100.86	52.22	5.11	36.4
G12	81.44	100.85	44.99	4.96	29.1
G13	82.39	100.85	39.67	4.40	25.7
G14	82.10	100.86	34.80	4.09	17.8
G15	81.97	100.92	31.10	3.49	14.0
G21	81.81	100.76	43.48	4.72	33.9
G22	81.44	100.85	44.99	4.96	29.1
G23	81.95	100.91	50.18	5.08	27.7
G24	83.02	100.88	54.76	5.49	25.7
G25	81.56	100.87	59.17	5.91	24.9

2.3.2. Analysis of Cutting Strength

To establish the relationship between drilling parameters V_s, F_p, N_r, M_q and rock mass strength parameters, the cutting mechanics analysis model is established by the rock cutting and fracture characteristics F_c is the force of cutting edge on the rock, F_f is the horizontal force acting on the rock by the cutting edge bottom, and T is the force to break the rock. The resultant moment of the force T on all cutting edges to the center is the drilling torque M_q. θ is the angle between Ff and the vertical line, ω is the inclination of cutting edge, ρ is the angle between the cutting force F_c and the cutting edge normal, as shown in Figure 5.

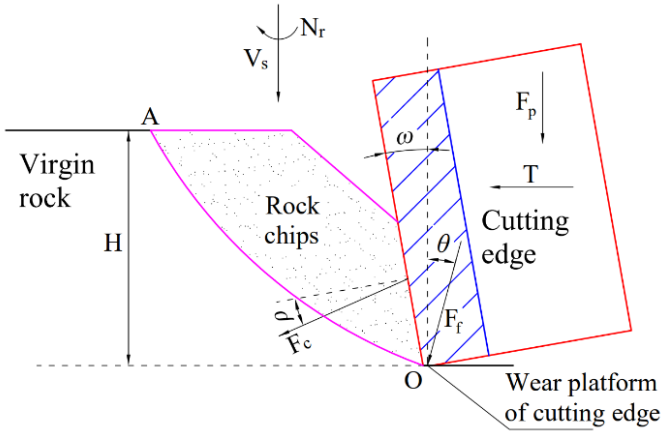

Figure. 5 Rock cutting mechanics analysis model.

The mechanical analysis is carried out with the cutting analysis model. The radius of the digital analytic bit is R, with n rows of cutting edges; L_i is the cutting-edge length in column i. In this paper, the numerical of the size parameters of the digital analytic bit is as follows: R=30mm，L_1=27mm、L_2=18mm、L_3=18mm. Conduct force analysis on any row of cutting edges, the torque of any micro segment dr in the cutting edge is as follows:

$$dM_q = \left[F_C' \cos(\omega + \rho) + F_f' \sin\theta\right] r dr \quad (1)$$

where $F_c^{'}$ is the reaction of the cutting edge to cutting force, and $F_f^{'}$ is the friction force on the cutting edge. The inclination of cutting edge ω is 15°. The values of angles θ and ρ are both 12° [26, 27]. dM_q is integrated along the length of the cutting edge, and the torques of the three rows of cutting edges are added. The relationship between torque M_q and parameters while drilling is obtained as follows:

$$M_q = \frac{1}{2}\left[F_C' \cos(\omega + \rho) + F_f' \sin\theta\right](2R\sum_{i=1}^{n} L_i - \sum_{i=1}^{n} L_i^2) \tag{2}$$

The drilling pressure F_p generated by the bit during drilling is as follows:

$$F_p = \left[F_C' \cos(\omega + \rho) + F_f' \sin\theta\right]\sum_{i=1}^{n} L_i \tag{3}$$

Equations (2) and (3) are combined to eliminate the friction force $F_f^{'}$ exerted by the rock on the cutting edge. The ultimate cutting force F_c of rock mass reinforced by cement slurry is obtained as follows:

$$F_c = \frac{2M_q - F_p tan\theta\left(2R - \sum_{i=1}^{n} L_i^2 / \sum_{i=1}^{n} L_i\right)}{[cos(\omega+\rho) - sin(\omega+\rho)tan\theta]\left(2R\sum_{i=1}^{n} L_i - \sum_{i=1}^{n} L_i^2\right)} \tag{4}$$

The cutting strength S_{cg} of grouted rock mass is defined as the ultimate cutting force required by the drill to cut grouted rock mass per unit volume. The relationship between cutting strength S_{cg} of grouting rock mass and parameters while drilling is obtained as follows:

$$S_{cg} = \frac{3N_r\left[2M_q - F_p tan\theta\left(2R - \sum_{i=1}^{n} L_i^2 / \sum_{i=1}^{n} L_i\right)\right]}{V_s[cos(\omega+\rho) - sin(\omega+\rho)tan\theta]\left(2R\sum_{i=1}^{n} L_i - \sum_{i=1}^{n} L_i^2\right)} \tag{5}$$

Combined with the drilling test of grouted rock mass carried out in this paper, the drilling parameters of V_s, F_p, N_r and M_q during the drilling process are obtained, as shown in Table 2. The drilling parameters are substituted into Equation (5) and the cutting strength S_{cg} of grouted rock mass is obtained, as shown in Table 3.

Table 3 Statistics of calculation results of rock cutting strength

Specimens number	S_{cg} **/MPa**
G11	120.91
G12	96.84
G13	83.99
G14	70.34
G15	65.59
G21	94.24
G22	96.84
G23	114.49
G24	124.13
G25	136.86

3. Response analysis of rock mass while drilling

3.1. The characteristics of drilling parameters

Through the analysis of test results in Table 2, the response law of drilling parameters to water-cement ratio and rock particle sizes is shown in Figures 6-7. In order to quantitatively analyze the response law of drilling parameters, the variable index of drilling parameters η is established.

$$\eta = \frac{q_{max} - q_{min}}{q_0} \times 100\% \quad (6)$$

where q_{max}、q_{min} are the maximum and minimum values of the monitored parameters respectively, and q_0 is equivalent to q_{max}.

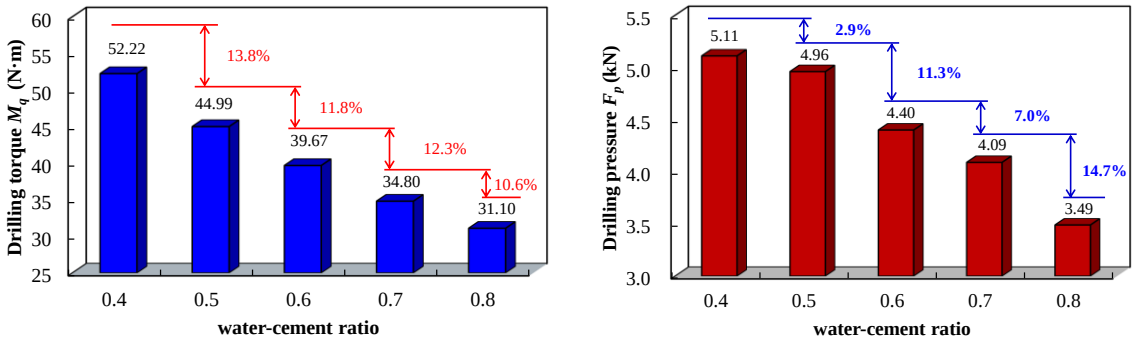

(A) (B)

Figure. 6 The response law of drilling parameters with different water-cement ratio. (A) The response law of drilling torque M_q, (B) The response law of drilling pressure F_p.

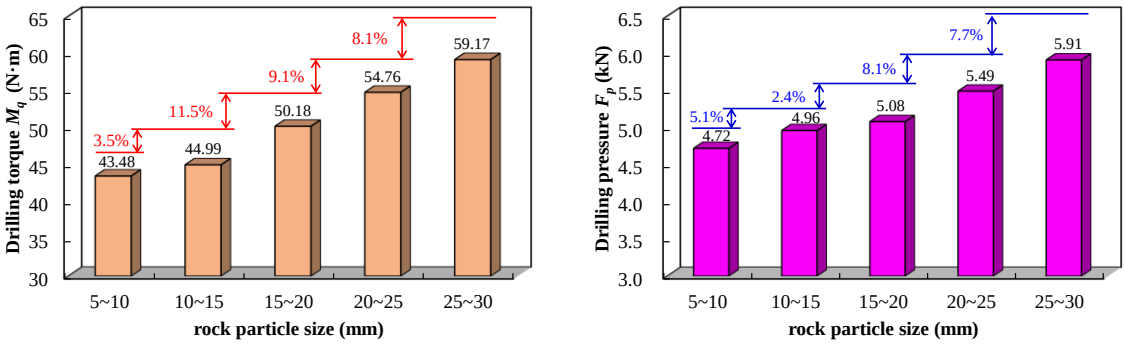

(A) (B)

Figure. 7 The response law of drilling parameters with different rock particle sizes. (A) The response law of drilling torque M_q, (B) The response law of drilling pressure F_p.

From the analysis in Figure 6, the drilling torque M_q and drilling pressure F_p decrease as the water-cement ratio increase. When the water-cement ratio increases from 0.4 to 0.8, the values of M_q are 52.55 N·m, 44.99 N·m, 39.67 N·m, 34.8 N·m, and 31.1 N·m, respectively; They decreased by 13.8%, 11.8%, 12.3%, and 10.6% respectively. The values of F_p were 5.11kN, 4.96kN, 4.4kN, 4.09kN, and 3.49kN, respectively, a decrease of 2.9%, 11.3%, 7.0%, and 14.7%. The average decrease in M_q was 12.13%, with a decrease of over 10%. The average decrease in F_p was 8.98%. The variable indexes η of M_q and F_p are 40.44% and 31.70% respectively. Compared with F_p, M_q is more significant responsive to the change of water-cement ratio.

From the analysis in Figure 7, the drilling torque M_q and drilling pressure F_p increase with the increase of rock particle size. When the rock particle size gradually increases from 5-

10mm to 25-30mm, M_q is 43.48 N·m, 44.99 N·m, 50.18 N·m, 54.76 N·m, and 59.17 N·m, respectively; It increased by 3.5%, 11.5%, 9.1%, and 8.1% respectively. F_p is 4.72kN, 4.96kN, 5.08kN, 5.49kN, and 5.91kN respectively; They increased by 5.1%, 2.4%, 8.1%, and 7.7% respectively. The average change rates of M_q and F_p were 8.05% and 5.83%, respectively. The variable indexes η of M_q and F_p are 26.52% and 20.14%. respectively. Compared to F_p, M_q is more responsive to the change of rock particle sizes.

3.2. The characteristics of cutting strength

In order to analyze the response law of cutting strength S_{cg} of different water-cement ratio and rock particle sizes, the histogram of cutting strength S_{cg} of different water-cement ratio and rock particle sizes is plotted, as shown in Figure 8.

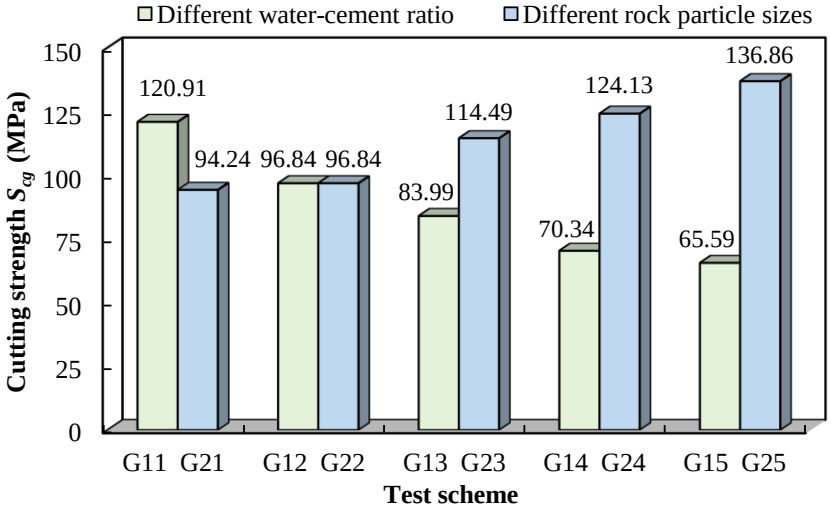

Figure. 8 The response law of S_{cg} with different water-cement ratio and rock particle sizes.

In order to quantitatively analyze the response law of cutting strength, the variable index of cutting strength υ is established.

$$\upsilon = \frac{x_{max} - x_{min}}{x_0} \times 100\% \tag{7}$$

where x_{max}、x_{min} are the maximum and minimum values of the cutting strength, and x_0 is equivalent to x_{max}.

The cutting strength S_{cg} of rock mass decreases with the water-cement ratio increase. When the water-cement ratio gradually increases from 0.4 to 0.8, S_{cg} decreases by 19.9%, 13.3%, 16.3%, 6.8% respectively. The water-cement ratio increases from 0.4 to 0.5, 0.5 to 0.6, and 0.6 to 0.7, S_{cg} decreases significantly, and the reduction of S_{cg} is all more than 10%. When the water-cement ratio increases from 0.7 to 0.8, the reduction rate of S_{cg} is only 6.8%. Compared with the first four groups, the change of S_{cg} is smaller. As shown in Figure 8, the variable index υ of S_{cg} is 45.75% under different water-cement ratio conditions.

The cutting strength S_{cg} generally increases with the rock particle sizes increase. When rock particle sizes gradually change from 5-10 mm to 25-30 mm, S_{cg} increases by 2.8%, 18.2%, 8.4%, 10.3% respectively. Compared with the last three groups, the change of S_{cg} is less obvious when rock particle sizes increase from 5-10mm to 10-15mm. As shown in Figure 8,

the variable index υ of S_{cg} is 31.14% under different rock particle sizes conditions. Compared with the rock particle sizes, the cutting strength S_{cg} is more responsive to the change of water-cement ratio.

3.3. The response law of compressive strength

In order to analyze the response law of different water-cement ratio and rock particle sizes compressive strength, the variation curves of compressive strength σ_c with water-cement ratio and rock particle sizes are plotted, as shown in Figures 9 and 10.

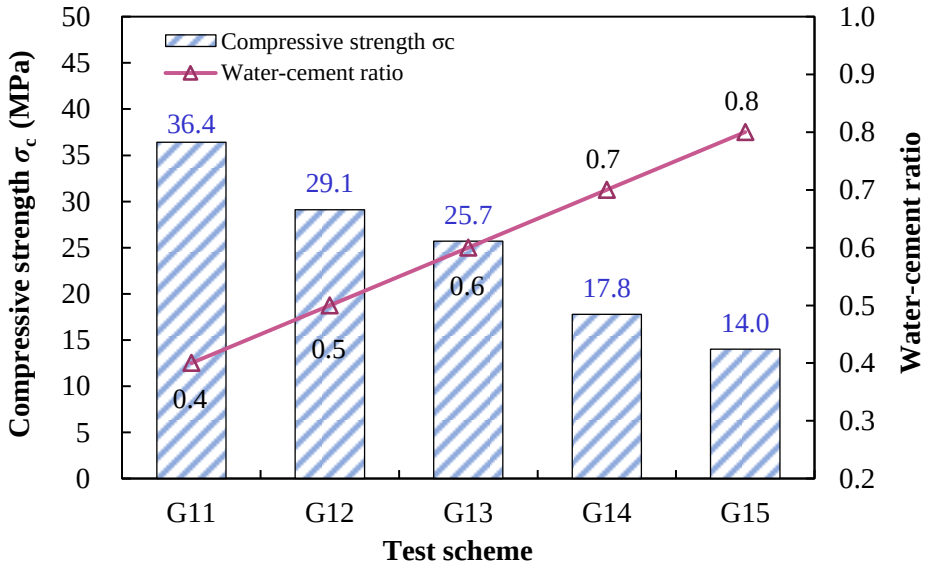

Figure. 9 The response law of σ_c with different water-cement ratio.

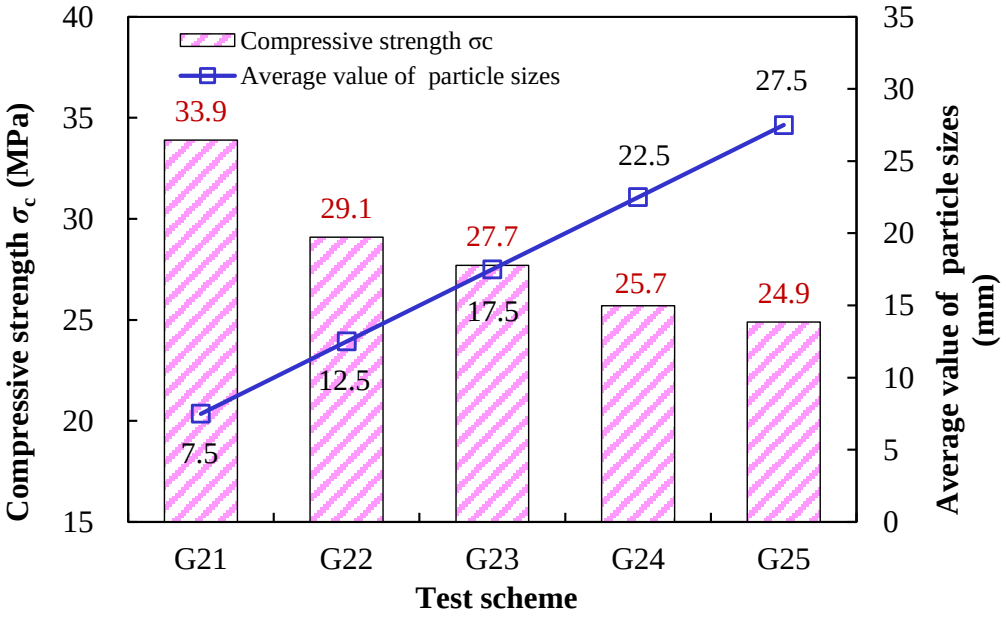

Figure. 10 The response law of σ_c with different rock particle sizes.

In order to quantitatively analyze the response law of compressive strength, the variable index of compressive strength ψ is established.

$$\psi = \frac{y_{max} - y_{min}}{y_0} \times 100\% \quad (8)$$

where y_{max}、y_{min} are the maximum and minimum values of the compressive strength, and y_0 is equivalent to y_{max}.

The rock mass compressive strength σ_c decreases as both the water-cement ratio and average rock particle sizes increase, respectively. When the water-cement ratio gradually increases from 0.4 to 0.8, the differences of σ_c are 7.3, 3.4, 7.9, 3.8 respectively. The reduction rates are 20.1%, 11.7%, 30.7%, 21.3% respectively. As shown in Figure 9, the variable index ψ of σ_c is 61.54%. σ_c changes significantly when the water-cement ratio increases from 0.6 to 0.7. When rock particle sizes gradually change from 5-10 mm to 25-30 mm, S_{cg} decreases by 14.2%, 4.8%, 7.2%, 3.1% respectively. As shown in Figure 10, the variable index ψ of σ_c is 26.55%. σ_c decreases with the increase of rock particle sizes. Compared with the water-cement ratio, the compressive strength σ_c is less responsive to the change of rock particle sizes.

4. Establishment of model to test rock compressive strength based on drilling

Under the conditions of the same rock particle size and different water-cement ratio, the variation law of cutting strength S_{cg} and compressive strength σ_c of slurry reinforced rock mass is consistent. There is a positive correlation between S_{cg} and σ_c. It shows that it is possible to obtain the strength of slurry reinforced rock mass by using cutting strength.

Under different rock particle sizes, S_{cg} increased with the particle sizes increase. However, σ_c decreased with the particle sizes increase. When the rock particle size is larger, the contact area between the cutting edge and the fragment in specimen is larger in the same cutting range. Because the strength of rock is greater than that of cement slurry, S_{cg} showed an increasing trend with the increase of rock particle size. It indicated that S_{cg} is related to the broken degree of rock mass before grouting. According to the uniaxial compression test results of rock mass, the strength of cementation surface between broken rock and cement slurry is low. Rock specimen is mainly damaged along the weak contact surface between broken rock and cement slurry. With the rock particle sizes increase, the weak contact surface in the specimen is larger. Therefore, compressive strength σc decreased with the rock particle sizes increase. Under the condition of different rock particle size, the grouting rock mass strength and drilling parameters show different variation trends.

On the basis of the tests carried out in this paper, combined with the test data of slurry reinforced rock mass with particle size of 10 ~ 15mm and different water-cement ratio, the quantitative relationship between grouting rock mass strength and drilling parameters is studied. Different formula fitting analysis is carried out for σ_c and S_{cg} of grout reinforced rock mass, as shown in Figure 11.

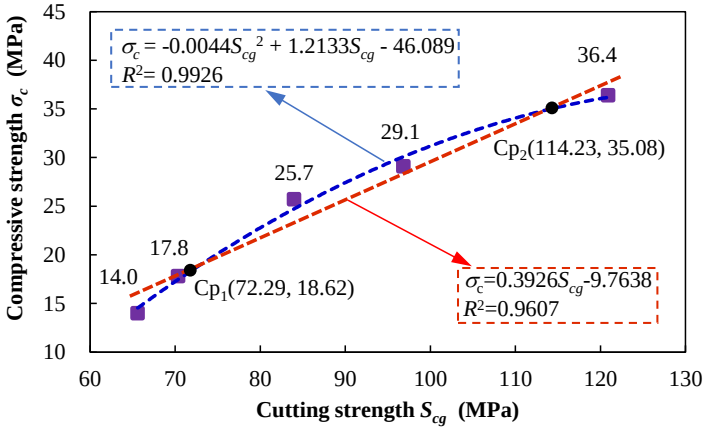

Figure. 11 The relationship between S_{cg} and σ_c of rock mass reinforcedby cement slurry.

(1) The relationship between σ_c and S_{cg} is analyzed by linear fitting. The goodness of fit R^2 is 0.9607. The fitting equation is as follows:

where, p_1 is drilling cutting coefficient. p_1=0.3926. n_1 is the drilling cutting constant. n_1=-9.7638.

$$\sigma_c = p_1 S_{cg} + n_1 \tag{9}$$

(2) The relationship between σ_c and S_{cg} is analyzed by polynomial fitting. The goodness of fit R^2 is 0.9926. The fitting equation is as follows:

$$\sigma_c = kS_{cg}^2 + p_2 S_{cg} + n_2 \tag{10}$$

where, k and p_2 are drilling cutting coefficients. k=-0.0044 and p_2=1.2133. n_2 is drilling cutting constant. n_2=-46.089.

According to the analysis of Figure 11, the linear fitting curve and polynomial fitting curve intersect at the points C_{p1} (72.29, 18.62) and C_{p2} (114.23, 35.08). The difference rate between two fitted curves is low. The accuracy of the fitting relationship between the two methods reflected in this range is similar. The fitting relationship can be adopted a simpler linear regression equation, as follows:

$$\sigma_c = p_1 S_{cg} + n_1 = 0.3926 S_{cg} - 9.7638 \tag{11}$$

where: $S_{cg} = \frac{3N_r[2M_q - F_p tan\theta(2R - \sum_{i=1}^{n} L_i^2 / \sum_{i=1}^{n} L_i)]}{V_s[\cos(\omega+\rho) - \sin(\omega+\rho)tan\theta](2R\sum_{i=1}^{n} L_i - \sum_{i=1}^{n} L_i^2)}$

The drilling test model of the grouting rock mass strength parameters and above drilling parameters is established. The results of rock samples compressive strength is 18.62MPa-35.08MPa. In the future research, the drilling tests of slurry reinforced rock mass under different broken conditions will be widely carried out, and the testing model of grouting rock mass drilling parameters and strength parameters should be improved. Based on the relationship between grouting rock mass strength and drilling parameters, a method for evaluating the grouting rock mass strength while drilling is proposed. The method is divided into the following two steps.

(1) The field drilling test of slurry reinforced rock mass is carried out by using field digital drilling test system. Drilling rate V_s, rotational speed N_r, drilling torque M_q, and drilling pressure F_p are monitored in real time.

(2) The above parameters are brought into the while-drilling testing model to obtain the strength σ_2 after grouting reinforcement, and compare it with the rock mass strength σ_1 before grouting reinforcement at the adjacent position of the same borehole to obtain the increase rate of rock mass strength ζ.

$$\zeta = \frac{\sigma_2 - \sigma_1}{\sigma_1} \times 100\% \quad (12)$$

where σ_1 is the rock strength before grouted; σ_2 is the rock strength after grouted.

5. Conclusion

(1) The drilling tests of rock mass reinforced by cement slurry with different water-cement ratio and rock particle sizes are carried out with the developed rock digital drilling test system. The cutting strength of rock mass reinforced by cement slurry specimens is obtained based on the rock cutting mechanical model. The response law of different water-cement ratio and rock particle sizes on drilling parameters, cutting strength, and rock mass strength parameters are analyzed.

(2) Under the condition of different water-cement ratio, the variation law of drilling parameters, cutting strength and compressive strength are consistent with the water-cement ratio. It indicates that the feasible method for evaluating the grouting rock mass is to obtain the grouting rock mass strength through drilling parameters.

(3) The cutting strength S_{cg} of grouting rock mass increases with the particle sizes increase. The compressive strength σ_c decreases with the increase of rock particle sizes. It indicates that S_{cg} is related to the fragmentation degree of rock mass before grouting. Under the condition of different rock particle sizes, the drilling parameters and the strength parameters of rock mass reinforced by cement slurry show different variation trends.

(4) The quantitative relationship between drilling parameters and strength parameters of rock mass reinforced by cement slurry is established, based on the relationship analysis of compressive strength σ_c and cutting strength S_{cg}. In future research, drilling tests of grouting rock mass with different strength and broken degree need to be carried out, and improve the relationship between rock mass strength and drilling parameters.

Acknowledgments: This work was supported by the China National Postdoctoral Program for Innovative Talents (grant number BX20220341); and the Project funded by China Postdoctoral Science Foundation (grant number 2022M713382).

Conflict of interest: The authors declare that they have no known competing financial interests or personal relationships that could have appeared to influence the work reported in this paper.

References:

1. Zhu C., Xu Y, Wu Y, et al. A hybrid artificial bee colony algorithm and support vector machine for predicting blast-induced ground vibration, *Earthq. Eng. Eng. Vib.*, 2022, 21, 861-876. DOI: 10.1007/s11803-022-2125-0
2. Li X, Li Q, Hu Y, et al. Study on Three-Dimensional Dynamic Stability of Open-Pit High

Slope under Blasting Vibration, *Lithosphere*, 2021, 4, 6426550. DOI: 10.2113/2022/6426550

3. Ren D, Wang X, Kou Z, et al. Feasibility evaluation of CO_2 EOR and storage in tight oil reservoirs: A demonstration project in the Ordos Basin, *Fuel*, 2023, 331, 125652. DOI: 10.1016/j.fuel.2022.125652
4. Lin P, Zhu X, Li Q, et al. Study on optimal grouting timing for controlling uplift deformation of a super high arch dam, *Rock Mech. Rock Eng.,* 2016, 49, 115-142. DOI: 10.1007/s00603-015-0732-z
5. Wang Q, Jiang Z, Jiang B, et al. Research on an automatic roadway formation method in deep mining areas by roof cutting with high-strength bolt-grouting, *Int. J. Rock Mech. Min.*, 2020, 128, 104264. DOI: 10.1016/j.ijrmms.2020.104264
6. Yin Q, Wu J, Jiang Z, et al. Investigating the effect of water quenching cycles on mechanical behaviors for granites after conventional triaxial compression, *Geomech. Geophys Geo.*, 2022, 8, 77. DOI: 10.1007/s40948-022-00388-0
7. Funehag J, Gustafson G, Design of grouting with silica sol in hard rock-new methods for calculation of penetration length, Part I, *Tunn. Undergr. Space Technol.* 2008, 23(1), 1-8. DOI: 10.1016/j.tust.2006.12.005
8. Zhang M., Fan X, Zhang Q, et al. Parametric sensitivity study of wellbore stability in transversely isotropic medium based on polyaxial strength criteria, *J. Pet. Sci. Eng.*, 2021, 197: 108078. DOI: 10.1016/j.petrol.2020.108078
9. Zhang M, Fan X, Zhang Q, et al. Influence of multi-planes of weakness on unstable zones near wellbore wall in a fractured formation, *J. Nat. Gas Sci. Eng.,* 2021, 93: 104026. DOI: 10.1016/j.jngse.2021.104026
10. Wang Q, Xu S, Xin Z, et al. Mechanical properties and field application of constant resistance energy-absorbing anchor cable, *Tunn. Undergr. Space Technol.* 2022, 125: 104526. DOI: 10.1016/j.tust.2022.104526
11. Wang Y, Zhu C. He M, et al. Macro-meso dynamic fracture behaviors of Xinjiang marble exposed to freeze thaw and frequent impact disturbance loads: a lab-scale testing, *Geomech. Geophys Geo.*, 2022, 8(5), 154. DOI: 10.1007/s40948-022-00472-5
12. Zong Y, Han L, Han G, Mechanical characteristics of confined grouting reinforcement for cracked rock mass, *J. Min. Saf. Eng.*, 2013, 30(4), 483-488.
13. Sun Z, Li S, Liu R, et al. Quantitative research on grouting reinforcement of soft fluid-plastic stratum, *Chin. J. Rock Mech. and Eng.*, 2016, 35(1), 3385-3393. DOI: 10.13722/j.cnki.jrme.2015.1152
14. Lu H, Zhang Q, Investigations on shear properties of soft rock joints under grouting, *Rock Mech. Rock Eng.,* 2021, 54, 1875-1883. DOI: 10.1007/s00603-021-02366-6
15. Salimian M, Baghbanan A, Hashemolhosseini H, et al. Effect of grouting on shear behavior of rock joint, *Int. J. Rock Mech. and Min*, 2017, 98, 159-166. DOI: 10.1016/j.ijrmms.2017.07.002
16. Wang Q, Qu L, Guo H, et al. Grouting reinforcement technique of qingdao jiaozhou bay subsea tunnel, *Chin. J. Rock Mech. Eng.*, 2011, 30(4), 790-802.
17. Liu Q, Zhou Y, Lu C, et al. Experimental study on mechanical properties of mudstone fracture before and after grouting, *J. Min. Saf. Eng.*, 2016, 33(3), 509-514+520. DOI:

10.13545/j.cnki.jmse.2016.03.020

18. Chen M, Lu W, Zhang W, et al. An analysis of consolidation grouting effect of bedrock based on its acoustic velocity increase, *Rock Mech. Rock Eng.*, 2014, 48(3), 1259-1274. DOI: 10.1007/s00603-014-0624-7
19. Wang D, Zhang Q, Zhang X, et al. Research and application on tunnel and underground engineering grouting effect of the fuzzy evaluation method, *Chin. J. Rock Mech. and Eng.*, 2017, 36(1), 3431-3439. DOI: 10.13722/j.cnki.jrme.2016.0232
20. Chen J, and Yue Z, Ground characterization using breaking-action-based zoning analysis of rotary-percussive instrumented drilling, *Int. J. Rock Mech. Min.*, 2015, 75, 33-43. DOI: 10.1016/j.ijrmms.2014.11.008
21. He M, Li N and Zhang Z, An empirical method for determining the mechanical properties of jointed rock mass using drilling energy, *Int. J. Rock Mech. Min.*, 2019, 116, 64-74. DOI: doi.org/10.1016/j.ijrmms.2019.03.010
22. Wang Q, Qin Q., Gao H, et al. A testing method for rock c-φ parameter based on digital drilling test technology, *J. China Coal Soc.*, 2019, 44(3), 915-922. DOI: 10. 13225/j.cnki.jccs.2018.0674
23. He M, Li N, Wu J, et al. Advanced prediction for field strength parameters of rock using drilling operational data from impregnated diamond bit, *J. Pet. Sci. Eng.*, 2020, 187, 106847. DOI: 10.1016/j.petrol.2019.106847
24. Wang Q, Gao H, Jiang B, et al. Relationship model for the drilling parameters from a digital drilling rig versus the rock mechanical parameters and its application, *Arab. J. Geosci.* 2018, 11, 357. DOI: 10.1007/s12517-018-3715-z
25. Gao H, Wang Q, Jiang B, et al. Relationship between rock uniaxial compressive strength and digital core drilling parameters and its forecast method, *Int. J. Coal Sci. Tech.*, 2021, 8(4), 605-613. DOI: 10.1007/s40789-020-00383-4
26. Huang H, Lecampion B, Detournay E, Discrete element modeling of tool-rock interaction I: rock cutting, *Int. J. Nume.r Ana.l Methods Geomech.* 2013, 37(3), 1913-1929. DOI: 10.1002/nag.2113
27. Yahiaoui M, Paris JY, Delbé K, *et al*. Independent analyses of cutting and friction forces applied on a single polycrystalline diamond compact cutter, *Int. J. Rock Mech. Min.,* 2016, 85, 20-26. Doi: 10.1016/j.ijrmms.2016.03.002